Title

Marine microbes rapidly adapt to consume ethane, propane, and butane within the dissolved hydrocarbon plume of a natural seep

Journal

Journal of Geophysical Research - Oceans, 120(3)

ISSN

2169-9275

Authors

Mendes, Stephanie D
Redmond, Molly C
Voigritter, Karl
et al.

Publication Date

2015-03-01

DOI

10.1002/2014jc010362

Peer reviewed

AGU PUBLICATIONS

JGR

Journal of Geophysical Research: Oceans

RESEARCH ARTICLE

10.1002/2014JC010362

Key Points:
- Developed a tritium tracer method to track microbial oxidation of natural gas
- Demonstrated rapid microbial response to ethane, propane, and butane

Correspondence to:
D. L. Valentine,
valentine@geol.ucsb.edu

Citation:
Mendes, S. D., M. C. Redmond, K. Voigritter, C. Perez, R. Scarlett, and D. L. Valentine (2015), Marine microbes rapidly adapt to consume ethane, propane, and butane within the dissolved hydrocarbon plume of a natural seep, *J. Geophys. Res. Oceans*, *120*, doi:10.1002/2014JC010362.

Received 2 AUG 2014
Accepted 11 FEB 2015
Accepted article online 18 FEB 2015

Marine microbes rapidly adapt to consume ethane, propane, and butane within the dissolved hydrocarbon plume of a natural seep

Stephanie D. Mendes[1], Molly C. Redmond[1,2,3], Karl Voigritter[4], Christian Perez[2], Rachel Scarlett[2], and David L. Valentine[1,2]

[1]Department of Earth Science, University of California at Santa Barbara, Santa Barbara, California, USA, [2]Marine Science Institute, University of California at Santa Barbara, Santa Barbara, California, USA, [3]Now at Department of Biological Sciences, University of North Carolina at Charlotte, Charlotte, North Carolina, USA, [4]Department of Chemistry and Biochemistry, University of California at Santa Barbara, Santa Barbara, California, USA

Abstract Simple hydrocarbon gases containing two to four carbons (ethane, propane, and butane) are among the most abundant compounds present in petroleum reservoirs, and are introduced into the ocean through natural seepage and industrial discharge. Yet little is known about the bacterial consumption of these compounds in ocean waters. To assess the timing by which microbes metabolize these gases, we conducted a three-phase study that tested and applied a radiotracer-based method to quantify the oxidation rates of ethane, propane, and butane in fresh seawater samples. Phase 1 involved the synthesis of tritiated ethane, propane, and butane using Grignard reagents and tritiated water. Phase 2 was a systematic assessment of experimental conditions, wherein the indigenous microbial community was found to rapidly oxidize ethane, propane, and butane. Phase 3 was the application of this tritium method near the Coal Oil Point seeps, offshore California. Spatial and temporal patterns of ethane, propane, and butane oxidation down current from the hydrocarbon seeps demonstrated that >99% of these gases are metabolized within 1.3 days following initial exposure. The oxidation of ethane outpaced oxidation of propane and butane with patterns indicating the microbial community responded to these gases by rapid adaptation or growth. Methane oxidation responded the slowest in plume waters. Estimates based on the observed metabolic rates and carbon mass balance suggest that ethane, propane, and butane-consuming microorganisms may transiently account for a majority of the total microbial community in these impacted waters.

1. Introduction

Thermogenic hydrocarbon gases generated in the deep subsurface are among the most abundant compounds in petroleum deposits. For example, ethane, propane, and butane together accounted for ~9% of the mass discharged from the Macondo well during the Deep water Horizon event, the most abundant individual compounds after methane [*Reddy et al*., 2012]. The emission of hydrocarbon gases into the ocean and atmosphere can have significant environmental repercussions. Understanding the interplay between physical and microbiological controls is the motivation for this research.

Ethane, propane, and butane biogeochemistry is relatively unstudied compared to methane, which serves as an important benchmark for comparison. Methane is the most abundant of these gaseous hydrocarbons and the most potent as a greenhouse gas [*Cicerone and Oremland*, 1988; *Etiope et al*., 2008; *Fung et al*., 1991]. Current estimates suggest that 75–310 Tg of methane is released into the ocean each year, but only ~10 Tg of that methane reaches the atmosphere [*Reeburgh*, 2007]. The majority of methane is consumed by marine microorganisms, which act as an effective biofilter [*Reeburgh*, 2007].

Ethane, propane, and butane are also greenhouse gases [*Collins et al*., 2002] and precursors to atmospheric pollutants such as acetone, alkyl nitrates, and ozone [*Jacob et al*., 2002; *Katzenstein et al*., 2003; *Singh et al*., 1994]. Their emissions from the ocean are estimated as 0.54, 0.35, and 0.11 Tg/yr, respectively [*Plass-Dulmer et al*., 1995]. However, natural seep environments were not considered in these estimates and may provide an important contribution. For example, the Coal Oil Point seep field in the Santa Barbara Channel releases

0.005 Tg/yr of ethane and propane, equivalent to ~1% of ocean emissions, with only half of this discharge reaching the atmosphere as bubbles rising to the sea surface [*Clark et al*., 2000]. The remainder of the gas dissolves into the water column and is transported away from the seep by ocean currents [*Mau et al*., 2010, 2007]. The partitioning of the dissolved gas between atmospheric flux and biological consumption remains uncertain.

The biogeochemical importance of these gases has been highlighted by a series of recent industrial incidents. In 2010, the Deep water Horizon well blowout in the Gulf of Mexico caused the world's largest accidental marine oil discharge. In addition to oil, an estimated 1.7×10^{11} g of natural gas was released into the ocean over 85 days [*Reddy et al*., 2012]. The event was noteworthy not only because of its scale, but also because the oil and gas were discharged to the ocean at a depth of 1500 m. At this depth, virtually all the ethane, propane, and butane dissolved into the water column. Ethane and propane (and probably butane) were consumed by bacteria within weeks after discharge [*Valentine et al*., 2010], with propane alone accounting for up to ~60% of total respiration in some samples. While the importance of ethane, propane, and butane during subsea discharge events is now recognized, there is still minimal understanding as to the factors responsible for a microbial response. Even after the Deepwater Horizon event, the continued occurrence of petroleum spills [*Coast Guard, United States*, 2013] and gas blowouts in particular (e.g., Elgin field blowout in the North Sea and the Hercules 265 blowout in the Gulf of Mexico) demonstrate that such events happen frequently enough to argue for an improved understanding of the oceanographic effects of ethane, propane, and butane discharge.

Microbial oxidation is a major control on the atmospheric release of oceanic methane, ethane, propane, and butane. Marine bacteria are known to oxidize these gases and are presumed to do so by first converting the hydrocarbon to its analogous alcohol and water, followed by conversion to carbon dioxide, biomass, and additional water [*Arp*, 1999; *Ashraf et al*., 1994; *Hanson and Hanson*, 1996; *Perry*, 1980], as shown in equations (1)–(4). Previous studies have focused on the biochemistry of methane oxidation and the ecology of responsible bacteria [*Hanson and Hanson*, 1996; *Reeburgh*, 2007; *Valentine*, 2011]. Comparatively few studies have considered ethane, propane, and butane consumption, particularly in the marine realm. For example, the anaerobic oxidation of methane (AOM) has been studied since the late 1960s [*Reeburgh*, 1969], whereas the anaerobic oxidation of ethane, propane, and butane has only recently been investigated [*Adams et al*., 2013; *Mastalerz et al*., 2009; *Kniemeyer et al*., 2007; *Quistad and Valentine*, 2011].

$$\text{Methane}: \quad CH_4 + 2O_2 \rightarrow \{CH_3OH\} \rightarrow CO_2 + 2H_2O + \{\text{Biomass}\}, \tag{1}$$

$$\text{Ethane}: \quad C_2H_6 + 3.5O_2 \rightarrow \{C_2H_5OH\} \rightarrow 2CO_2 + 3H_2O + \{\text{Biomass}\}, \tag{2}$$

$$\text{Propane}: \quad C_3H_8 + 5O_2 \rightarrow \{C_3H_7OH\} \rightarrow 3CO_2 + 4H_2O + \{\text{Biomass}\}, \tag{3}$$

$$\text{Butane}: \quad C_4H_{10} + 6.5O_2 \rightarrow \{C_4H_9OH\} \rightarrow 4CO_2 + 5H_2O + \{\text{Biomass}\}. \tag{4}$$

One critical factor for predicting the impact of ethane, propane, and butane input to the ocean is understanding the response of the microbial community. This specifically pertains to the timeframe for adaptation of the microbial community to respire these gases. ^{13}C-labeled tracers have been used to measure propane oxidation rates in anoxic sediments of a hydrocarbon seep as well as ethane and propane oxidation rates after the Deep water Horizon oil spill [*Quistad and Valentine*, 2011; *Valentine et al*., 2010]. However, the ^{13}C-tracer method is relatively insensitive and its utility is limited to environments where the ambient gas concentrations are high and the conversion of ^{13}C is detectable above background levels of dissolved inorganic carbon. In most environments, a more sensitive tracer is required to effectively quantify oxidation rates.

Herein, we developed and applied a tritium-based tracer method for quantifying respiration rates for ethane, propane, and butane. Our methods were modeled after the tritiated methane method of *Reeburgh et al*. [1991] as modified by *Valentine et al*. [2001]. This study reports new experimental techniques and applications to natural samples with the goal of tracking microbial oxidation of ethane, propane, and butane dissolved into the ocean. These experiments are described in three phases: Phase 1, synthesis of tritiated hydrocarbon tracers; Phase 2, tests of the tracer's efficacy for quantifying hydrocarbon respiration rate in fresh seawater samples; Phase 3, tritium tracer application for tracking spatial and temporal patterns of hydrocarbon oxidation after exposure at a natural hydrocarbon seep.

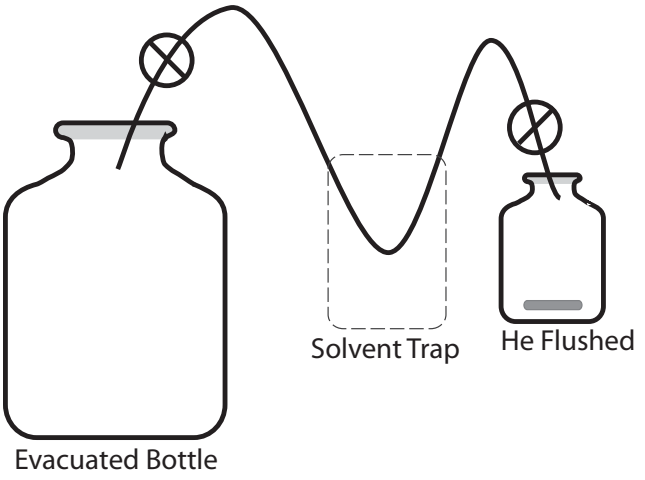

Figure 1. Schematic for synthesis of tritium-labeled hydrocarbon gases. The synthesis occurred in the He-flushed reaction bottle, and any gas produced was transferred to an evacuated collection bottle. The solvent trap (dry ice and acetone) was used to remove any residual organic solvent or water from the synthesized gas.

2. Method

2.1. Synthesis (Phase 1)

Tritiated tracers were synthesized using Grignard reagents and tritiated water. All reactions were performed using oven-dried glassware under an atmosphere of dry helium. The Grignard reagents ethylmagnesium bromide, propylmagnesium chloride, and butylmagnesium bromide are commercially available from Sigma Aldrich and were used as received (2 *M* in tetrahydrofuran). Tritiated water (a mixture of H_2O and HTO) was purchased from Moravek Biochemicals (20.83 Ci/mL in dry tetrahydrofuran). All reactions were performed in 5 mL serum bottles sealed with chlorobutyl rubber stoppers. The resulting gases were transferred to 12 mL serum bottles using 1/16″ OD stainless steel tubing attached to two valves (Figure 1). Concentrations were measured using a gas chromatograph coupled to a flame ionization detector and activity was determined with a Beckman LS6500 liquid scintillation counter, with associated errors of 6 n*M* and 0.2 nCi, respectively.

2.1.1. Representative Tritium Labeling Procedure: Ethane-1-*t*

The general experimental procedure was adapted from a deuterium-labeling synthesis outlined in *Olszowy and Kitching* [1984] (equations (5)–(8)).

An ethylmagnesium bromide solution (100 μL, 0.2 mmol) was added to an oven dried, He-purged 5 mL serum bottle sealed with a butyl rubber stopper via a dried syringe. The solution was cooled to 0°C, and the tritiated water solution (68 μL, 0.08 mmol) was added dropwise. The reaction was allowed to warm to room temperature and was stirred overnight. The tritiated gas was then transferred to an evacuated bottle for storage. This was carried out using a dry custom-made Swagelok transfer line consisting of 1/16″ OD stainless steel tubing equipped with two-way stainless steel valves on each end (Figure 1). The gas was passed through a "solvent trap," which consisted of a portion of the transfer line being immersed in a dry ice/acetone cooling bath to trap any residual tetrahydrofuran.

$$\text{General}: \quad \mathrm{R{-}MgX{+}HTO} \rightarrow \mathrm{R{-}H \ or \ R{-}T}, \tag{5}$$

$$\text{Ethane}: \quad \mathrm{C_2H_5{-}MgBr{+}HTO} \rightarrow \mathrm{C_2H_5T \ or \ C_2H_6}, \tag{6}$$

$$\text{Propane}: \quad \mathrm{C_3H_7{-}MgCl{+}HTO} \rightarrow \mathrm{C_3H_7T \ or \ C_3H_8}, \tag{7}$$

$$\text{Butane}: \quad n\mathrm{{-}C_4H_9{-}MgBr{+}HTO} \rightarrow \mathrm{C_4H_9T \ or \ C_4H_{10}}. \tag{8}$$

2.2. Method Assessment (Phase 2)

2.2.1. Method Assessment Study Site

Samples were collected from the *R/V Atlantis* in September 2011. Water for the method assessment study was collected during one cast of a 24 bottle Niskin rosette at station Plume 3 (Table 1 and Figure 2), 10.5 km down-current from Coal Oil Point. For reference, Coal Oil Point emits $>10^{10}$ g/yr of natural gas with a composition of 87.5% methane, 5.1% ethane, and 3.1% propane, along with trace amounts of heavier hydrocarbons [*Clark et al*., 2000; *Mau et al*., 2010]. Though these seeps are relatively shallow (ranging from 5 to 80 m) [*Hornafius et al*., 1999], *Clark et al*. [2000] calculated that 3.6×10^6, 2.1×10^5, 1.2×10^5, and 3.7×10^4 mol d^{-1} of methane, ethane, propane, and butane, respectively, are dissolved into the water. Of that, only 1% of methane and less than 1% of ethane and propane is transferred to the atmosphere in the immediate vicinity of the seeps [*Mau et al*., 2010, 2013].

Table 1. Background Chemical and Physical Conditions of the Water Mass Sampled for the Method Assessment Experiment on 21 September 2011[a]

Depth (m)	Temperature (°C)	Density (kg/m^3)	Salinity	O_2 (mL/L)	O_2 (% saturation)	[C_1H_4] (n*M*)	[C_2H_6] (n*M*)	[C_3H_8] (n*M*)	[C_4H_{10}] (n*M*)
40	11.95	1025.45	33.29	4.44	72	2100	77	51	10

[a]The location is identical to station Plume 3 from Table 2.

2.2.2. Tritium Tracer Method

The method for ethane, propane, and butane oxidation rate measurements was adapted from previously published procedures for methane [*Reeburgh et al*., 1991; *Valentine et al*., 2001]. The five general steps are as follows: (1) collect seawater samples in 160 mL serum bottles, seal with a chlorobutyl stopper and metal crimp cap, take replicates for ambient concentration measurement, (2) add tritiated gas to samples via gas-tight syringe and incubate, (3) add mercuric chloride (0.5 mL of a saturated water solution) to halt further consumption of the tracer and sparge with a nonradioactive gas, such as air, to remove any unreacted tracer (4) measure activity in the sample (amount of tracer consumed) using a liquid scintillation counter (LSC), (5) calculate rate of microbial consumption using equations (9)–(13). For kill controls, Step 3 is done prior to Step 2.

Methane oxidation rates were also measured during the method assessment as a comparison, using the same five steps outlined. Samples were injected with 10 μCi of methane tracer (100 μL of 0.1 Ci/L tritiated methane stock) and incubated for 24 h near in situ temperature.

2.2.3. Ambient Hydrocarbon Concentration Analysis

Ambient concentrations of dissolved methane, ethane, propane, and butane were determined using established techniques [*Heintz et al*., 2012; *Mau et al*., 2010; *Valentine et al*., 2001]. Seawater samples were transferred to 160 mL serum bottles, and dissolved gas from the sample bottle was exsolved by replacing 10 mL of seawater with 10 mL of ultrapure N_2 gas. To inhibit microbial activity, mercuric chloride was added to all samples intended for concentration analysis. Samples were shaken vigorously and allowed to equilibrate for a minimum of 12 h. Headspace concentrations were measured with a gas chromatograph coupled to a flame ionization detector (GC-FID; Shimadzu Corp. 14A) and run isothermally (60°C) using N_2 as the carrier gas through a 12′ × 1/8″ packed column (n-octane on Res-Sil C). Analytical error from GC-FID measurements, based on previous application of this method, was ±5%.

2.2.4. Calculating Oxidation Rates

The fraction of hydrocarbon tracer converted to aqueous-phase product (f_{ox}) is calculated directly from the ratio of tracer consumed (activity of tritium in the aqueous phase, A_{aq}) to amount of tracer injected (total

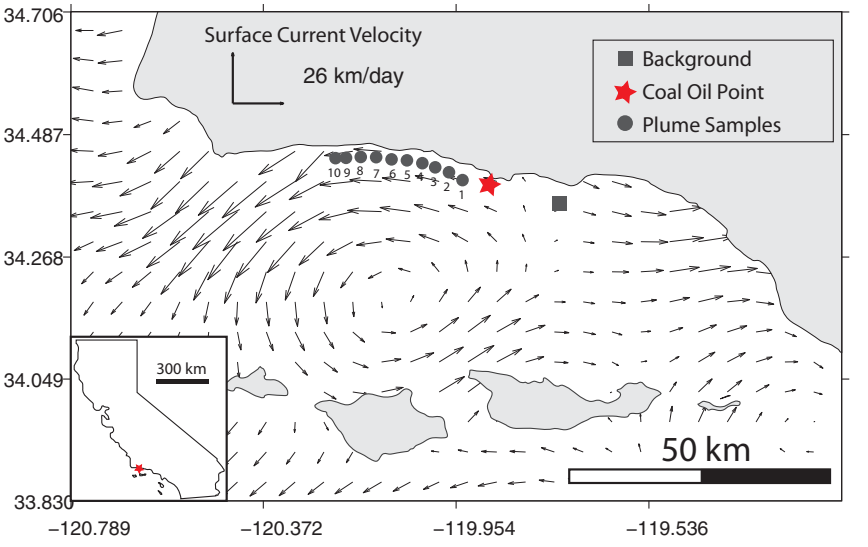

Figure 2. The Coal Oil Point seep field (represented by the red star) is located offshore Goleta, California. Arrows represent surface current velocities averaged during the plume sampling period from 23 July 2012 to 25 September 2012. The background sample (represented by the gray square) was collected outside of the seep area on 16 September 2011.

activity of tritium tracer injected, A_i), after accounting for abiotic contributions as quantified by kill controls (activity of tritium from abiotic sources, A_x).

$$f_{ox} = (A_{aq} - A_x)/(A_i - A_x). \quad (9)$$

Because A_x is typically very small compared to A_i, f_{ox} can be simplified as:

$$f_{ox} = (A_{aq} - A_x)/(A_i). \quad (10)$$

By accounting for the incubation time (t_i), the fractional turnover rate of tritium-labeled tracer (k') can be calculated as:

$$k' = f_{ox}/t_i. \quad (11)$$

Assuming the tracer behaves identically to the unlabeled substrate (i.e., complete mixing and no isotope effects), the average rate of substrate consumption in the sample (R_b) can be calculated from the molar concentrations of labeled substrate (concentration of tritium-labeled substrate added to the sample, S_T) and the initial substrate (concentration of substrate present in the sample at the time the tracer was injected, S_e):

$$R_b = k' * [S_T + S_e]. \quad (12)$$

For the sake of clarity, this study reports primarily the fractional turnover rate (k') as a metric of substrate consumption.

Under select conditions these equations can be expanded to calculate the in-situ oxidation rate of substrate (i.e., the rate at which substrate in the sample would be consumed if not removed from its natural environment, R_e), as is typically done for the calculation of methane oxidation rate [*Valentine et al.*, 2001]. Necessary conditions include: (1) oxidation rate is linearly dependent on the substrate concentration (first-order kinetic behavior), (2) the microbial community is neither in growth nor decline with respect to the substrate being studied, (3) the microbial community is not primed by the addition of exogenous substrate, and (4) the conditions of sampling and incubation do not affect the capacity of the microbial community to consume substrate. Thus the rate of substrate consumption may be expressed in a first-order form:

$$R_e = k' * [S_e]. \quad (13)$$

Note that results of this study deviate from the form of equation (13), and the significance of these deviations are considered in section 4.1. Replicate samples measured on the LSC had an average error of $\pm$0.2 nCi.

2.2.5. Comparison With Established ^{13}C Method

To compare sensitivity between ^{3}H and ^{13}C-tracer methods, oxidation rate experiments using both tracers were run in parallel for ethane and propane. Rate measurements with ^{13}C were performed using a similar approach to those reported by *Valentine et al.* [2010]. A small volume (5–100 μL) of 99% ^{13}C-labeled ethane or propane tracer was injected into each sample. Water samples were also collected for kill controls and background dissolved inorganic carbon (DIC) measurements. The ^{13}C of DIC in seawater was determined using the Finnigan Delta XP Isotope Ratio Mass Spectrometer (IRMS) coupled with the Finnigan Gas Bench. Oxidation rates are calculated using the same rate equation as the tritium approach (equation (13)); however, the fractional turnover rate is calculated using equations (14) and (15). These equations account for background ^{13}C found in seawater and the molar quantity of CO_2 produced from each tracer.

$$k = (\text{normalized moles of } CO_2)/((\text{incubation time}) * (\text{moles of tracer})), \quad (14)$$

$$\text{Normalized moles of } CO_2 = (\text{background moles of } CO_2 * (((\delta^{13}C_{rate\ sample}/1000)+1) * 0.0112372) - (((\delta^{13}C_{background}/1000)+1) * 0.0112372))/\text{number of carbons in tracer}. \quad (15)$$

2.3. Method Application—Oxidation Within a Plume (Phase 3)

2.3.1. Sample Collection

Seawater samples were collected in California's Santa Barbara Channel (Figure 2 and Table 2) from aboard the *R/V Atlantis* (September 2011) and the *M/V Connell* (June–September 2012). Identifying and tracking the

Table 2. Select Properties of Samples From the Hydrocarbon Plume

Station	Depth (m)	Date Collected	Latitude	Longitude	Distance From Coal Oil Point (km)	[CH4] (n*M*)
Background	20	16 Sep 2011	34.358000°	−119.772000°	−8.1	66
Coal Oil Point	20–50	17 Sep 2011	34.375000°	−119.853167°	0	2000
Plume 1	25	31 Jul 2012	34.401650°	−119.929720°	8	1300
Plume 2	35	31 Jul 2012	34.411720°	−119.950870°	10.5	1250
Plume 3	54	31 Jul 2012	34.417666°	−119.983936°	13	720
Plume 4	45	2 Aug 2012	34.423830°	−120.011500°	15.5	2500
Plume 5	45	2 Aug 2012	34.434870°	−120.035070°	18	1500
Plume 6	45	2 Aug 2012	34.443980°	−120.055200°	20.5	1600
Plume 7	35	2 Aug 2012	34.444690°	−120.073580°	23	150
Plume 8	35	25 Sep 2012	34.444717°	−120.100967°	25.5	350
Plume 9	50	25 Sep 2012	34.445983°	−120.128283°	28	740
Plume 10	50	25 Sep 2012	34.451610°	−120.144270°	30.5	720

dissolved plume was the greatest challenge associated with sample collection. Since the samples were collected as the currents flowed westward, north-south transects were conducted in an attempt to intersect the core of the plume. The plume's core was identified by collecting water at depths from 35 to 55 m at each station along the N-S transect and analyzing the samples for hydrocarbon content shipboard using a GC-FID. Seawater samples for subsequent analysis were collected only at the station and depth where the maximum hydrocarbon signal was observed for each N-S transect. The N-S transects were spaced ~1.5 km apart and samples from the plume's core were analyzed for dissolved hydrocarbon concentration and ethane, propane, and butane oxidation rates.

2.3.2. Oxidation Rates in the Plume

Oxidation rates were determined using the five steps described in section 2.2.2. The experimental conditions were determined based on the results from the method assessment experiments as follows: for ethane, samples were incubated with 2 μCi (140 n*M*) for 12 h near in situ temperature; for propane, samples were incubated with 1 μCi (50 n*M*) for 24 h near in situ temperature; for butane, samples were incubated with 2 μCi (35 n*M*) for 24 h near in situ temperature (Table 3). Each replicate was injected with 100 μL of diluted tracer (a mixture of tritiated stock and N_2 gas), allowing for consistent and reproducible injections across replicate bottles. Ethane, propane, and butane diluted stock concentrations were 0.02, 0.01, and 0.02 Ci/L, respectively.

3. Results

3.1. Tracer Synthesis and Chemical Stability (Phase 1)

Tritiated ethane, propane, and butane were successfully synthesized using tritiated water and ethylmagnesium bromide, propylmagnesium chloride, and butylmagnesium bromide. Percent yields of tritiated gas were calculated with reference to tritiated water substrate and specific activity of synthesis gas was quantified in Ci/L and converted to mCi/mmol of hydrocarbon (Table 3).

Following synthesis, the tracers were stored individually over an aqueous brine solution, which led to an increase of radioactivity in the aqueous solution over time, presumably because of hydrogen exchange between each hydrocarbon and water [*Bottinga*, 1969; *Horibe and Craig*, 1995]. Isotope exchange also occurs with storage of tritium-labeled methane and is likely catalyzed by radicals formed following the autoradiolytic cleavage of C-T bonds. The gradual loss of tracer activity to the aqueous phase during storage combined with tritium's half-life of 12.3 years limits the useful lifetime of any batch of tracer to a period of <10 years. To correct for the influence of abiotic exchange during use of the tracer, kill controls are needed to empirically determine the amount of tritium incorporated into the seawater in the absence of microbial consumption. Tracer activity was assessed regularly by methods described above to ensure that

Table 3. Summary of the Tracer Synthesis[a]

Tritiated Tracer	Yield (%)	Specific Activity (mCi/mmol)
^{3}H-Ethane	36	77
^{3}H-Propane	57	400
^{3}H-Butane	37	420

[a]Percent yield was calculated with respect to water substrate. Specific activity is reported in mCi/mmol of hydrocarbon.

Table 4. Incubation Conditions for Samples From the Plume Tracking

Tracer (^{3}H)	Activity (μCi)	Incubation Time (h)	Incubation Temperature (°C)
Ethane	2	12	11
Propane	1	24	11
Butane	2	24	11

the injected tracer quantity was correct. A bias in tracer concentration will propagate through equation (13) and yield an incorrect rate. Transfer and purification of the tracer stock is also recommended when the stock has gone unused for a period of several months.

3.2. Method Assessment (Phase 2)

The tritiated tracer oxidation rate method was tested with water collected at a single station in September 2011 (Table 1). Each hydrocarbon tracer was evaluated for microbial response by varying: (1) the quantity of tritium-labeled substrate in the sample (i.e., activity), (2) the length of time for which each individual sample was incubated (i.e., incubation time), and (3) the temperature at which the sample was incubated (i.e., temperature). This ^{3}H tracer method was also compared to a previously utilized ^{13}C method [*Valentine et al.*, 2010]. Results from the method assessment experiments are shown in Figures 3–5. Methane had a fractional turnover rate of 9.6×10^{-4} day^{-1} (turnover time of ~3 years) and an oxidation rate of 2.0 n*M* d^{-1}, while ethane, propane, and butane had fractional turnover rates of 0.24, 0.17, and 0.71 day^{-1} (turnover times of ~4, 6, and 1.5 days), respectively, and oxidation rates of 20, 8.7, and 7.1 n*M* d^{-1}, for the same incubation conditions. For reference, samples subjected to an incubation period of 24 h have a maximum measurable fractional turnover rate of 1 day^{-1}; for samples subject to an incubation period of 12 h, the maximum measurable fractional turnover rate is 2 day^{-1} (i.e., complete substrate consumption after the incubation period).

3.2.1. Kill Controls

Control experiments were conducted by treating a subset of samples with saturated mercuric chloride to halt biological activity. Comparing killed to nonkilled samples, only a small amount of product is generated by abiotic reactions (Figure 6). Any activity found in the kill controls can thus be subtracted out as baseline and attributed to abiotic tritium exchange.

3.2.2. Activity

For ethane, the fractional turnover rate increased with increasing activity of tracer, most notably between the 1 and 2 μCi treatments. A discrepancy between duplicate samples treated with 4 μCi of tracer does not allow differentiation between two possible trends (Figure 3a): a continued linear increase in the fractional turnover rate with added tracer or a plateau in the turnover rate above 2 μCi. A linear increase is consistent with bacterial adaptation or growth, whereas a plateau is consistent with first-order kinetic behavior. Based on these results, samples were incubated with 2 μCi of ethane for subsequent application of the method (Table 4). Two microcurie was chosen to provide both a consistent response and a measureable level of tritium in the metabolic products.

Propane and butane fractional turnover rates increased linearly when tracer was varied from 1 to 2 and 1 to 4 μCi, respectively, with the exception of duplicates at 2 μCi for butane (Figures 3b and 3c). This linear behavior is reflective of an adaptive response, suggesting that increasing levels of tracer affected the metabolic capacity of the community. Fractional turnover rate reached a maximum of 0.35 day^{-1}

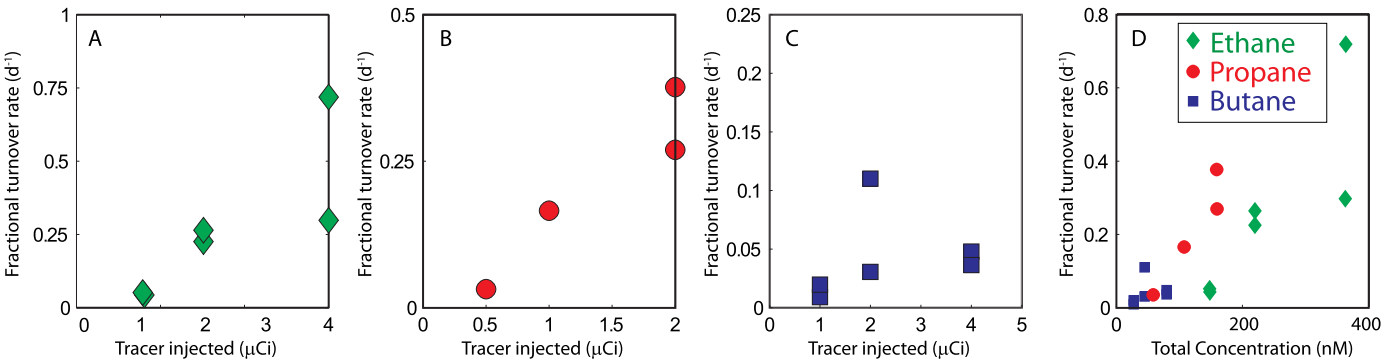

Figure 3. Response of the microbial community to addition of different quantities of tracer: (a) ethane, (b) propane, and (c) butane. (d) Total concentration of gas in bottle versus fractional turnover rate. All treatments were incubated at 11°C for 24 h. Duplicates are shown for each quantity of tracer injected, but some are too similar to be visually distinguished.

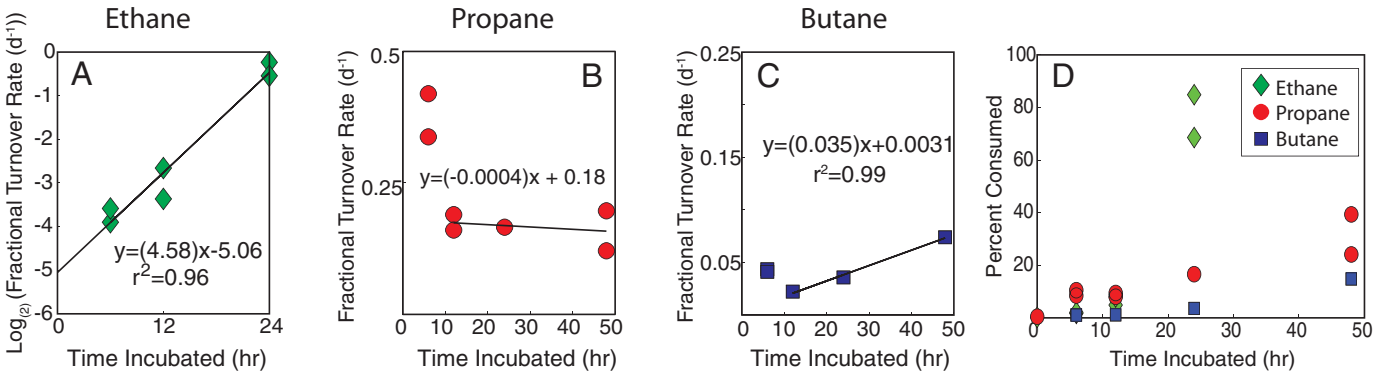

Figure 4. Incubation time response experiment conducted as part of the method assessment for (a) ethane: incubated at 11°C with 2 μCi of tracer, (b) propane: incubated at 11°C with 1 μCi of tracer, and (c) butane: incubated at 11°C with 2 μCi of tracer. (d) Incubation time series for ethane, propane, and butane showing the percent of tracer converted at different incubation times. Duplicates are shown for each sample interval. Regression in Figures 4b and 4c exclude the 6 h time point.

for propane and 0.05 day^{-1} for butane, except for butane's duplicate outlier that exceeded 0.1 day^{-1}. Divergence in the fractional turnover rate occurred at tracer additions $\geq$2 μCi. The molar quantity of tracer needed to achieve these activities was twelvefold greater than the ambient concentration, and the variability may represent inherent differences in growth or adaptive response. Based on these results, we opted to incubate samples with 1 μCi of propane or 2 μCi of butane for subsequent applications of these methods (Table 4). These quantities of tracer were chosen to provide measureable levels of tritium in the metabolic products.

A comparison of fractional turnover rate versus concentration for each hydrocarbon (Figure 3d) indicates an exponential relationship between the concentration and fractional turnover rate for each substrate, which is consistent with an adaptive response by the microbial community. These results further indicate that the microbial communities responded to the addition of ethane, propane, and butane, even at concentrations less than 50, 270, and 20 n*M*, respectively (Figure 3d).

3.2.3. Incubation Time

The fractional turnover rate for ethane increased exponentially over the course of 24 h (Figure 4a), presumably reflecting adaptation by the microbial population. After incubation for 24 h, the fractional turnover rate for ethane reached a value of 0.85 day^{-1}, approaching the empirical limit for this method. This exponential trend can be attributed to either of two distinct environmental factors: (1) an artificial response due to the added tracer or (2) population growth due to the naturally high ethane concentration introduced at the Coal Oil Point seeps. We favor a combination of these explanations wherein the microbial community began growing exponentially following exposure at Coal Oil Point and the addition of tracer prolonged this exponential phase. Based on the rapid adaptation for ethane, we opted to incubate samples for a period of 12 h for subsequent applications of this method (Table 4). This period of time was viewed as being sufficient to generate measureable levels of tritium in the metabolic products, but not so long as to stimulate complete consumption.

The time-course change in fractional turnover rates for propane and butane were distinctive compared to ethane. Both displayed decreases between 6 and 12 h of incubation, which is opposite the trend observed for ethane. Following 12 h of incubation, the fractional turnover rate for propane remained relatively constant or decreased slightly through the termination of the experiment at 48 h (Figure 4b). Butane's fractional turnover rate gradually increased during the time interval from 12 to 48 h (Figure 4c). Based on these results for propane and butane, we opted to incubate samples for a period of 24 h for subsequent applications of this method (Table 4).

The cause of the divergent trends for ethane versus propane and butane is not immediately apparent. Figure 4d highlights the coincidence in timing between the depletion of ethane and the increase in rate of consumption for propane and butane. While speculative, this timing is consistent with cometabolism of propane and butane by ethane-consuming bacteria.

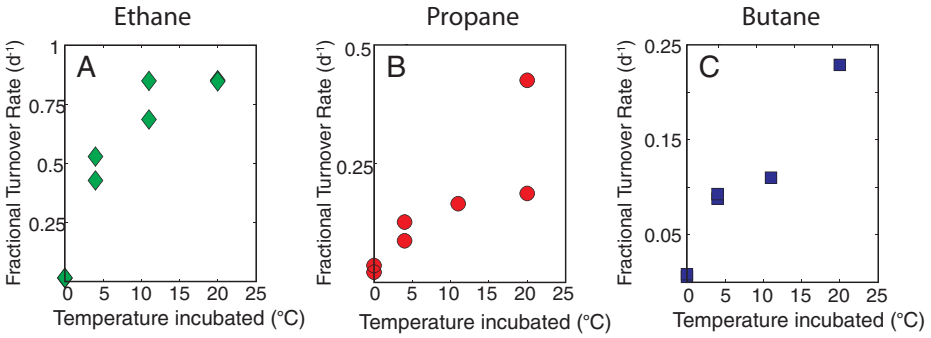

Figure 5. Temperature response experiment conducted as part of the method assessment for (a) ethane: incubated with 2 μCi of tracer for 24 h, (b) propane: incubated with 2 μCi of tracer for 24 h, and (c) butane: incubated with 2 μCi of tracer for 24 h. Duplicates are shown for each temperature.

3.2.4. Temperature

The impact of temperature on the fractional turnover rates for ethane, propane, and butane was assessed by incubating samples at 0, 4, 11, and 20°C, bracketing the ambient temperature of 11.5°C. The fractional turnover rate was found to increase with temperature in this range, for all treatments (Figure 5). The observed trends are typical for a marine microbial community and likely reflect a metabolic response to temperature.

3.2.5. ^{13}C Tracer and Substrate Concentration

A comparison of oxidation rates measured using the tritium method and ^{13}C-labeled ethane and propane revealed concentration dependence (Figures 7 and 8). A direct comparison between the two methods was hampered by this effect as the detection limit for ^{13}C in metabolic products required substrate concentrations from 3.3 to 30 μM, far above the ambient levels. The observed maximum oxidation rate occurred at tracer concentrations of 2.9–7.1 μM for both ethane and propane. Surprisingly, the oxidation rate decreased with increasing concentration beyond these maxima. This might suggest some form of inhibition at elevated substrate concentration. Alternatively, the two methods measure different metabolic products. The ^{3}H method measures all ^{3}H remaining in the sample, including the final product ($^{3}H_2O$) and all soluble ^{3}H-intermediates. The ^{3}H method, in effect, measures the rate of hydrocarbon loss in a sample, rather than the rate of product formation, whereas the ^{13}C method quantifies only the final carbon species of the oxidation pathway (CO_2). Results from the ^{13}C tracer application are consistent with a rate of incomplete metabolism or biomass accumulation that increases with substrate concentration in this range.

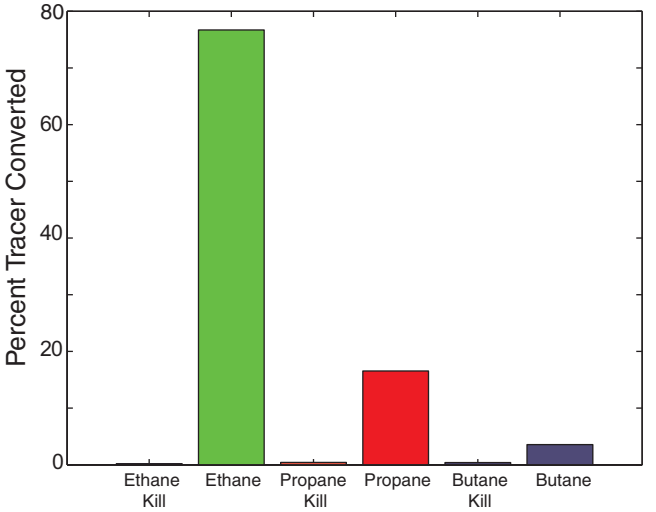

Figure 6. Comparison of tritiated ethane (green), propane (red), and butane (blue) converted during the kill control and rate incubation experiments collected for the method assessment (Table 1).

3.3. Tracking the Hydrocarbon Plume From Coal Oil Point (Phase 3)

The oxidation of ethane, propane, and butane was studied in the Santa Barbara Channel, within the down current plume of a hydrocarbon seep, in order to assess the in situ response of the marine microbial community to the input of these gases. This setting also provided context to the method assessment described above, during which all water had been collected at one location in this plume (station Plume 3). Monitoring currents with HF radar enabled tracking of hydrocarbon-laden waters from the seep field to a distance of 33 km down current, at which point plume features were lost (Figure 2 and

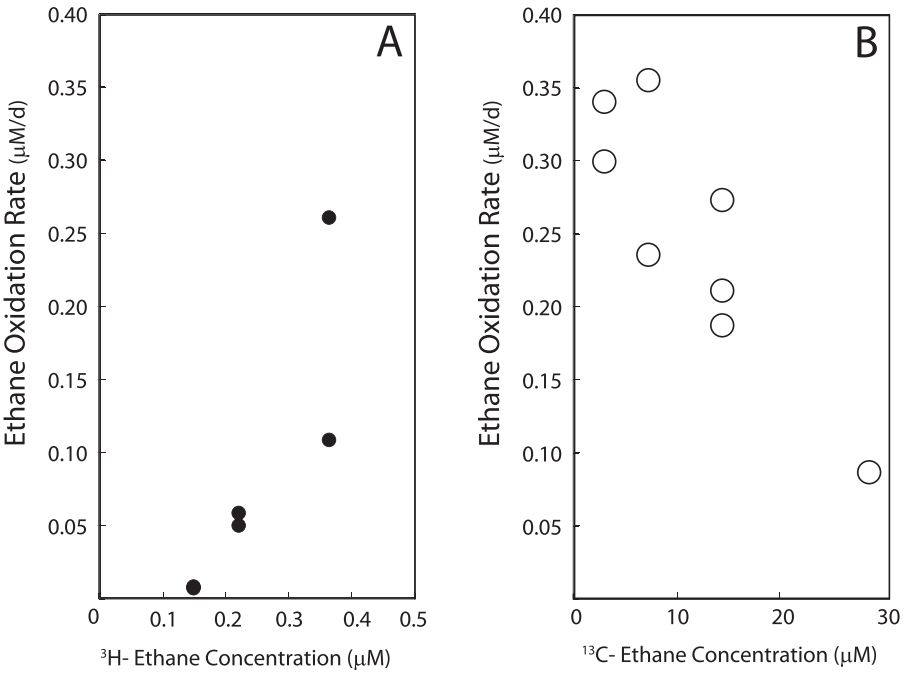

Figure 7. Ethane oxidation rates versus total concentration (ambient + tracer) in the bottle using (a) ^{3}H-ethane and (b) ^{13}C-ethane. Ambient ethane concentration was 77 n*M*. Note the different scales on the *x* axes.

Table 2). Methane was used to track the plume as its oxidation occurred slowly relative to the transit time of the water and no major seeps are known along the plume's path. Turnover time for methane was ~3 years compared to 3 days for the water to travel 33 km. Thus, methane was treated as a conservative tracer for hydrocarbon exposure.

Currents exhibited a counterclockwise rotation on all sampling days in the study area, common for the Santa Barbara Channel (Figure 2) [*Harms and Winant*, 1998]. As a result of this cyclonic motion, the dissolved

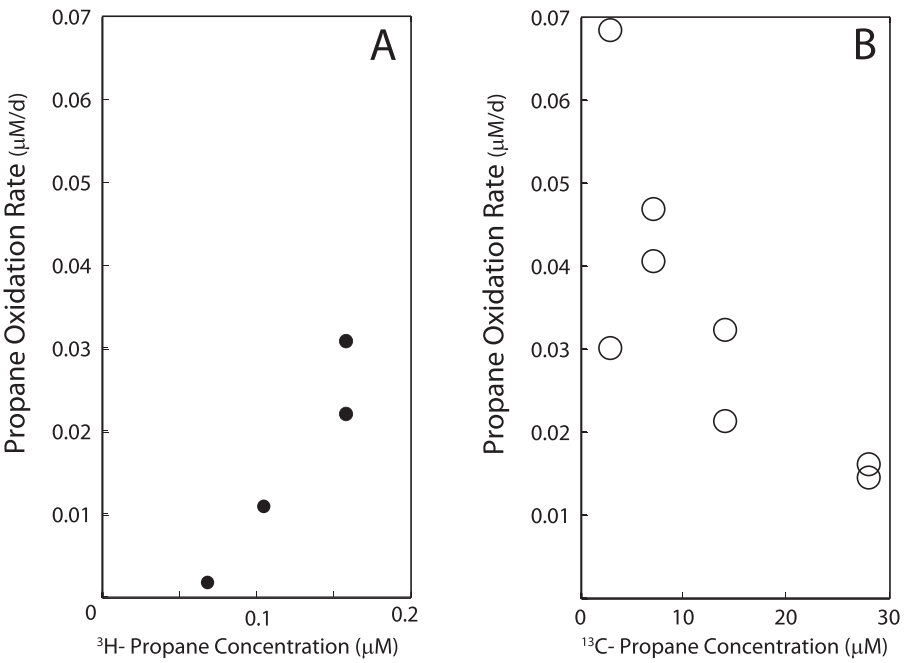

Figure 8. Propane oxidation rates measured versus total concentration (ambient + tracer) in the bottle using (a) ^{3}H tracer and (b) ^{13}C tracer. Ambient propane concentration was 51 n*M*. Note the different scales on the *x* axes.

hydrocarbon plume located on the north side of the basin traveled westward. The travel time between Coal Oil Point and stations within the dissolved plume were calculated by dividing the distance traveled by the current velocity. Current velocities taken during sampling intervals averaged 11.8 km/d (0.14 ± 0.05 m/s), which is consistent with previous studies [*Beckenbach*, 2004]. The travel time of water from the Coal Oil Point seep field to each station is expressed here in terms of time since exposure (TSE) using the average current velocity, as this term provides a clear metric for comparison to microbial adaptation. Note however that stations were sampled on different days and the results are not a true time series.

3.3.1. Hydrocarbon Gas Concentrations Within the Plume

The highest concentrations of ethane, propane, and butane (1750, 570, and 400 n*M*, respectively) were measured in samples collected at Coal Oil Point (station Plume 2). Concentrations generally decreased as the plume traveled with the current. Ethane, propane, and butane were no longer detectable (<1.5 n*M*) 1.5 days following exposure. Mixing within the plume samples was determined based on methane concentrations. Methane was considered to be a conservative tracer, oxidation rates observed were very low (turnover time of ~3 years), and the plume was located below the mixed layer depth [*Mau et al*., 2007]. Methane concentrations were variable within the plume (Table 2). In some cases, samples collected down current were more concentrated in methane than samples collected further up current. This behavior is expected for spot sampling of a dynamic feature and likely indicates the complexity in current flow and mixing. By treating methane as a conservative tracer, we were able to track the relative declines in ethane, propane, and butane (Figures 9c, 10c, and 11c), which we attribute to oxidation by bacteria in the plume. These results indicate that >99% of the ethane, propane, and butane were consumed within 1.3 days of exposure.

3.3.2. Fractional Turnover Rate Within the Plume

The impact of exposure on the fractional turnover rate was similar for each of the three gases tested (Figures 9a, 10a, and 11a). Low rates at the time of initial exposure gave way to higher rates down current, and then decreased back to low rates following substrate depletion. Ethane consumption occurred more rapidly than propane and butane consumption, reaching a maximum in samples collected 1.25 days following exposure, with a fractional turnover rate ≥2 day^{-1}. That is, 30 h following initial exposure, the microbial community was able to consume the entirety of added ethane tracer within a period of 12 h. Rates decreased down current in the absence of elevated ethane concentration until negligible tracer was removed from samples collected 2.75 days following initial exposure. This form of decay in the time course of activity may reflect both physical dilution of the microbial population and the response of the microbial community to ethane deprivation. Similarly, propane and butane consumption rates reached their maximums in samples collected 1.8 days following exposure and then decreased down current. The maximum

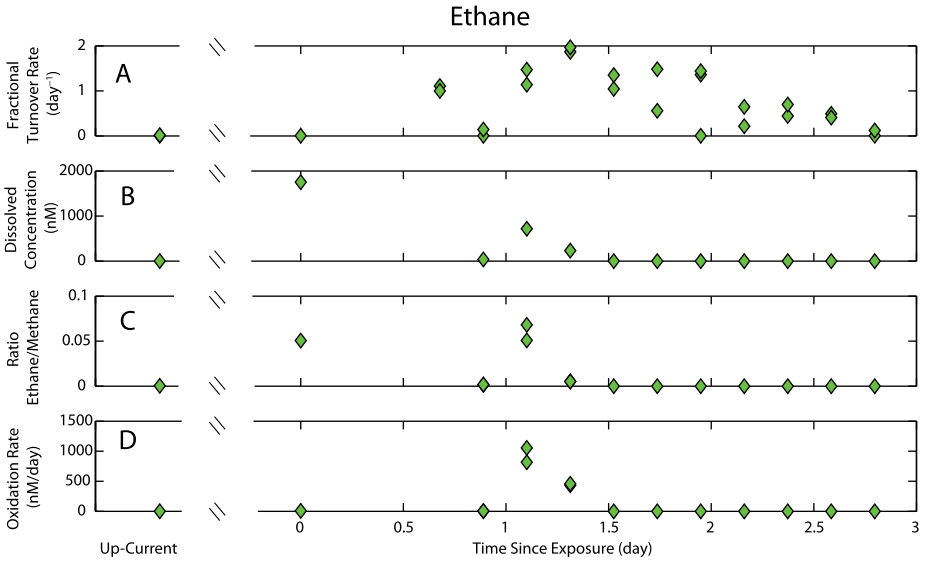

Figure 9. Ethane dynamics in the Coal Oil Point plume. (a) Ethane fractional turnover rate (day^{-1}). (b) Dissolved ethane concentration. (c) The ratio of dissolved ethane to methane. (d) Ethane oxidation rates. The *x* axis represents the minimum time traveled from Coal Oil Point, assuming a linear trajectory. Coal Oil Point is located at 0 day.

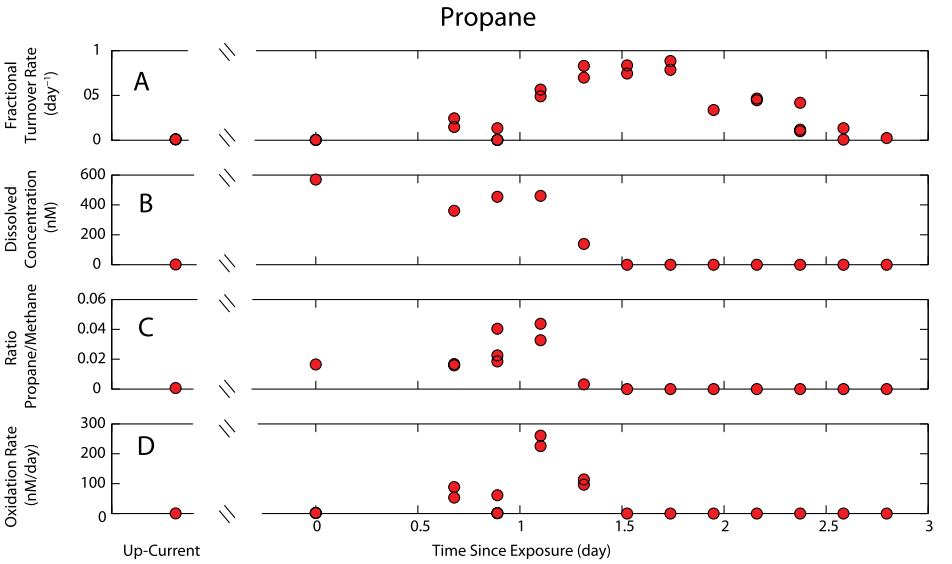

Figure 10. Propane dynamics in the Coal Oil Point plume. (a) Propane fractional turnover rate (day^{-1}). (b) Dissolved propane concentration. (c) The ratio of dissolved propane to methane. (d) Propane oxidation rates. The *x* axis represents the minimum time traveled from Coal Oil Point, assuming a linear trajectory. Coal Oil Point is located at 0 day.

rate of tracer removal was 0.89 day^{-1} for propane, while butane's fractional turnover rate never exceeded 0.2 day^{-1}. Butane consumption was sustained over the greatest time span with rates of tracer consumption averaging ~0.05 day^{-1} in samples collected 0.75–2.75 days following exposure. These results demonstrate that at Coal Oil Point, ethane, propane, and butane are consumed by the indigenous bacterial community within 2–3 days following exposure.

4. Discussion

4.1. Oxidation Rates and Kinetic Order

Conversion of radioisotope tracers as substrate to product is commonly used to estimate the rate of metabolism for a given set of conditions. The method described in this work is similar to that used for quantifying

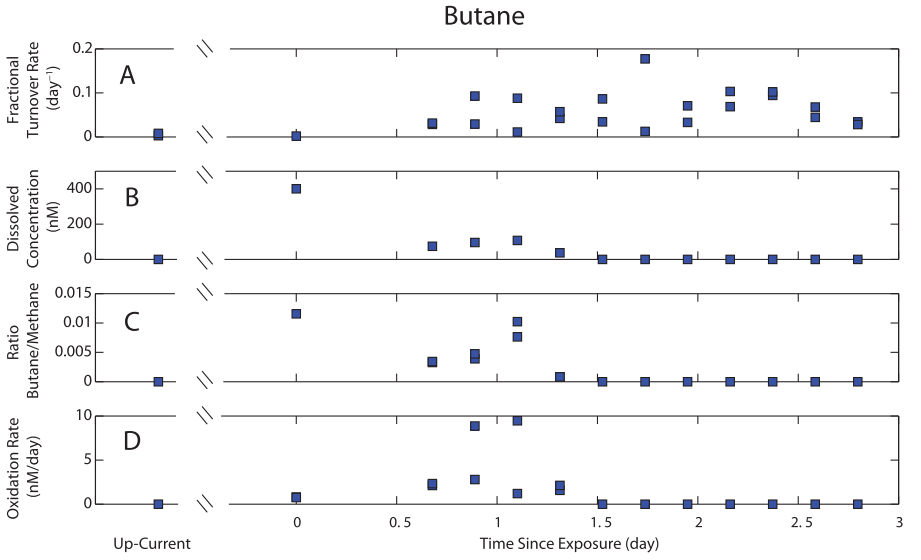

Figure 11. Butane dynamics in the Coal Oil Point plume. (a) Butane fractional turnover rate (day^{-1}). (b) Dissolved butane concentration. (c) The ratio of dissolved butane to methane. (d) Butane oxidation rates. The *x* axis represents the minimum time traveled from Coal Oil Point, assuming a linear trajectory. Coal Oil Point is located at 0 day.

methane oxidation rates [*Mau et al*., 2013; *Valentine et al*., 2001; *Ward et al*., 1987], wherein the transfer of tritium from methane to the aqueous phase is quantified following the incubation of a representative sample of seawater at conditions that approximate those experienced in situ by the microbial community. In the case of methane oxidation rate measurements, the low concentration of added methane (on the order of 10 n*M*) does not typically elicit a response in the microbial community [*Pack et al*., 2011; *Ward et al*., 1987] and is thus assumed to reflect the in situ rate of consumption. The results presented here demonstrate that microbial communities adapt more rapidly to the input of ethane, propane, or butane and require different treatments of the resulting data.

Results from the method assessment demonstrate that the quantity of tracer injected and the duration of the incubation impact the fractional turnover rate calculated from the incubations. These results violate the assumptions outlined in section 2.2.4 and illustrate several important differences between methane oxidation versus that of ethane, propane, and butane. First, the microbial community displays a clear adaptive response to the input of substrate wherein the addition of substrate primes metabolic rate (Figure 3). Second, ethane consumption by the microbial community displays an exponential rise during 24 h incubations (Figure 4a). This trend indicates rapid adaptation, though the data does not distinguish between the input of ethane at the seep versus the added tracer. Third, inconsistency in the trends observed for propane and butane (Figures 3 and 4) may relate to the fate of ethane introduced naturally from the seeps. Adaptation to ethane occurred rapidly compared to propane and butane. A substrate specificity that encompasses ethane, propane, and butane might explain the variability in the time course of propane and butane oxidation (Figures 4b and 4c). Given indications of an adaptive bacterial response to substrate input, we have not interpreted the results using a purely kinetic model. However, the results presented in Figures 7a and 8a indicate that the Michaelis-Menten model may aptly describe the rate's substrate response, for select experimental conditions. Interestingly, such an analysis indicates a first-order response to ethane and propane, but a zero-order response to butane.

Results from plume tracking studies are consistent with those from the method assessment. The microbial community adapted to consume ethane, propane, and butane within $\sim$1 day following exposure. This time scale frames the method assessment in a way that was not intended, in that samples used to assess the method were exposed to hydrocarbons on a similar time frame, indicating they may have been actively adapting to the hydrocarbon input at the time of sampling. Nonetheless, both the method assessment and the plume tracking studies reveal the same important trend: microbial adaptation to the input of ethane, propane, and butane occurs rapidly in this environment.

The rapid adaptive response of microbes to the input of ethane, propane, and butane limits the utility of kinetic expressions to describe the in situ rate of metabolism. Rates of hydrocarbon oxidation measured using isotope tracers are typically expressed as an in situ rate, a potential rate, or with a model such as Michaelis-Menten. The in situ rates are calculated as described in equation (13) and typically assume adherence to first-order kinetic behavior. Potential rates are calculated from conditions of elevated substrate concentration, at the point that the rate transitions to become zero order [*Reeburgh*, 1983; *Valentine et al*., 2010]. However, none of these kinetic behaviors accurately reflect an actively adapting or growing microbial community, which is expected to display an exponential increase in the rate of metabolism as the population of consumers increases.

Based on the results, we find the utility of oxidation rate measurements for ethane, propane, and butane to be restricted compared to those for methane. In the case of methane, such measurements are typically indicative of the microbes' in situ metabolic rate and are thus useful for calculating methane budgets under steady state conditions. For ethane, propane, and butane, such measurements are more indicative of the microbial communities' capacity to respond to the input of substrates into the environment. This distinction is rooted in the fundamentally more rapid response of ethane, propane, and butane degraders to the input of substrate when compared to methane degraders. Fractional turnover rates calculated from these tracer experiments provide a conservative representation of the in situ microbial condition, based on the expectations of kinetic models such as Michaelis-Menten. Further, given that the threshold concentration for consumption of methane is higher by a factor of 10 or more compared to ethane, propane, and butane, a more sensitive tracer method would be needed to calculate in situ rates for ethane, propane, and butane consumption at steady state conditions. The use of a higher-activity tritium label or a low-level ^{14}C tracer

coupled with accelerator mass spectrometry represent two potential approaches to limit the amount of additional substrate needed to calculate a rate measurement [*Pack et al.*, 2011].

4.2. Fate of Hydrocarbons in the Coal Oil Point Plume

Ethane, propane, and butane are oxidized more rapidly than methane; thus, the concentration of methane within the plume decreases more slowly than that of the other gases. By comparing the ratio of ethane/methane, propane/methane, and butane/methane, a shift toward methane is indicative of preferential microbial consumption [*Kinnaman et al.*, 2007; *Valentine et al.*, 2010]. Methane becomes more dominant as the plume travels down current, consistent with previous geochemical observations in the Santa Barbara Channel [*Clark et al.*, 2000; *Mau et al.*, 2007] (Figures 9c, 10c, and 11c). This trend is well supported by the rapid consumption rates observed within the plume (Figures 9d, 10d, and 11d).

Microbial response to the hydrocarbon plume emanating from Coal Oil Point shows the community's increased activity due to elevated substrate followed by a decrease due to substrate limitation. While substrates were still present within the plume, microbial consumption rates increased as hydrocarbon concentration decreased. As the plume aged and hydrocarbon concentrations fell below detection, fractional turnover rates began to drop. The longer the plume sustained hydrocarbon starvation, the lower the fractional turnover rates became. Even though all three gases had similar trends and reached their maximum consumption rate at 1.25 days, each gas maintained its maximum rate for a different duration (~1.25 days travel time for ethane, ~1.8 days for propane, ~2.5 days for butane; Figures 9–11). Ethane was consumed more quickly than propane or butane, which contrasts deep ocean samples and laboratory incubations that observed more rapid propane consumption compared to ethane [*Kinnaman et al.*, 2007; *Redmond et al.*, 2010].

4.3. Microbial Adaptation to Hydrocarbons

Data presented in the method assessment showed that ethane had a fractional turnover rate which increased exponentially over a 24 h period. This suggests that microbial growth was occurring over the course of the incubation (Figure 4a). This could be an artificial response to the added tracer or a population growth response to the naturally high hydrocarbon levels introduced at the Coal Oil Point seep. Samples for the method assessment experiment were collected 13 km from the plume's origin. Fractional turnover rates in the plume's water show that rates progressively increase as the water moves down current until reaching ~15.5 km (Figure 9a). Samples for the method assessment were collected up current from the observed maximum, and assuming similar current velocities and water mixing at the different times, we predict that microbial growth was likely due to the environmental response to the natural seep and not exclusively to the addition of tracer.

Hydrocarbon-consuming organisms typically make up a small fraction of the total open ocean bacterial community; however, when substrates are available, they can grow to dominate the community [*Harayama et al.*, 1999; *Margesin and Schinner*, 1999; *Redmond and Valentine*, 2012]. Only two studies have identified aerobic oxidizers of ethane and propane in marine environments [*Redmond et al.*, 2010; *Redmond and Valentine*, 2012]. In laboratory incubations with sediment collected near a natural thermogenic seep, *Redmond et al.* [2010] observed that ethane was primarily consumed by a group of organisms from the family Methylococcaceae, closely related to, but distinct from, the methane oxidizing Methylococcaceae observed in the same samples. Propane was primarily consumed by members of an unclassified Gammaproteobacterial group and was consumed more slowly than methane or ethane. In contrast, propane was oxidized more rapidly than ethane in hydrocarbon plumes formed during the 2010 Gulf of Mexico oil spill [*Valentine et al.*, 2010]. Both ethane and propane were initially consumed more rapidly than methane, though methane oxidation rates eventually increased enough that nearly all of the methane was consumed by bacteria [*Kessler et al.*, 2011; *Du and Kessler*, 2012]. Methylococcaceae were the dominant methane oxidizers, while ethane and propane oxidation was driven predominately by Colwellia [*Redmond and Valentine*, 2012].

Hydrocarbon oxidation in the Coal Oil Point water column is similar to the oil spill scenario in that ethane and propane oxidation increased more rapidly than methane oxidation following exposure. The present Coal Oil Point study differs in that ethane was oxidized more rapidly than propane. This may have been due

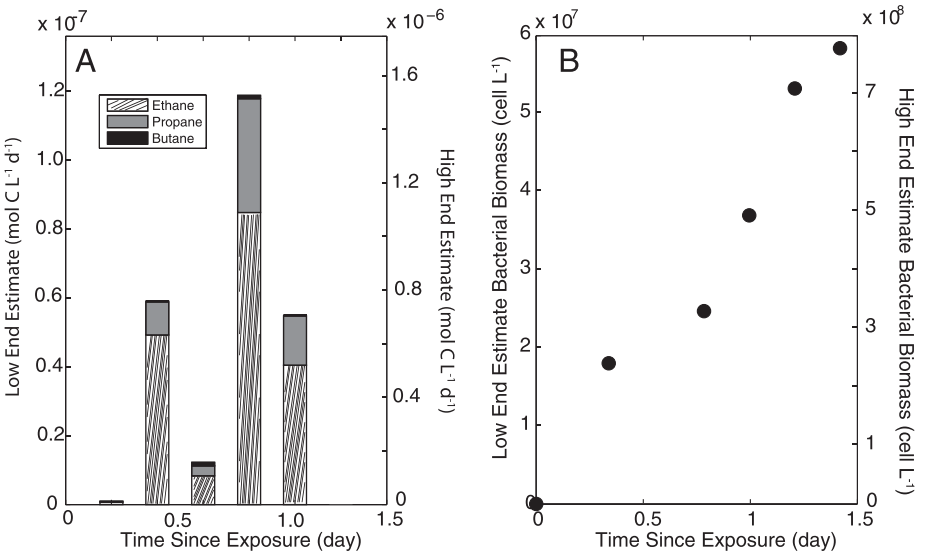

Figure 12. Estimates of microbial growth within the plume are calculated for (a) net bacterial production and (b) cumulative bacterial biomass from ethane, propane, and butane oxidizers. Growth efficiencies of 5% and 65% were used for the low-end and high-end estimates.

to more rapid growth by ethane oxidizers or to substrate preferences in bacteria that could oxidize ethane, propane, and butane. The much lower rates of methane oxidation suggest that this process was performed by other, slow-growing bacteria.

Since little is known about bacterial populations that consume ethane, propane, and butane in natural marine systems, we estimated the potential bacterial production from consumption of these hydrocarbons within the Coal Oil Point plume. Estimates of bacterial growth efficiencies are based on the reported range of 5%–65% for aerobic methanotrophs since equivalent data are sparse for consumers of ethane, propane, and butane [*Griffiths et al*., 1982; *Ward et al*., 1987]. Production estimates for the six stations with rates above background are shown in Figure 12a. The low-end estimates ranged between 0.0011×10^{-6} and 0.12×10^{-6} mol C L^{-1} d^{-1}, while the high-end estimates ranged between 0.014×10^{-6} and 1.7×10^{-6} mol C L^{-1} d^{-1}. In comparison, ^{3}H-Leucine incorporation measurements of net bacterial production in Santa Barbara Channel surface waters (35–55 m) typically range between 0.1×10^{-6} and 0.8×10^{-6} mol C L^{-1} d^{-1} (data courtesy of Craig Carlson and Emma Wear). Our estimates indicate that microbial production from hydrocarbon oxidation in the plume is equivalent to ~1% to ~213% of background microbial production. Similarly, the total bacterial biomass produced within the plume was calculated using a moving average approach for both the low and high-end net bacterial production estimates (Figure 12b). A carbon conversion factor of 15 fg C $cell^{-1}$ was used [*Halewood et al*., 2012]. Assuming no loss of cells as the plume travels down current, biomass accumulation within the plume ranges from 5.8×10^{7} to 7.6×10^{8} cell L^{-1}, indicating that a rapid bloom of hydrocarbon-degrading bacteria could account for up to ~68% of the microbial community in the affected waters, at least transiently.

5. Conclusion

Development of methods to quantify bacterial consumption of ethane, propane, and butane revealed a rapid and dynamic microbial response to hydrocarbon exposure, down current from a natural gas seep. The complete consumption of ethane, propane, and butane within 3 days of exposure is far more rapid than would be predicted based on methane's behavior and highlights the important distinction between the biogeochemistry of methane and other hydrocarbon gases. Significant gaps remain in our understanding of the environment's response to an irruption of natural gas that include the identities, physiologies, and distributions of major consumers; however, this work confirms our previous observation [*Valentine et al*., 2010] as to the Ocean's potential for a rapid microbial response.

Acknowledgments
Sampling and experimental efforts were aided by Christoph Pierre, Christian Orsini, David Salazar, Avi Rubin, Ryan Duncombe, as well as the Captain and crew of the *R/V Atlantis* during the SEEPS-11 expedition. Georges Paradis conducted stable isotope analyses, and Emma Wear and Craig Carlson provided bacterial production data. Susan Mau and John Pohlman provided constructive reviews of the manuscript. Contact corresponding author David Valentine (valentine@geol.ucsb.edu) to request any data presented in this work. Surface current velocity measurements are available online from the Southern California Coastal Ocean Observing System (SCCOOS; http://www.sccoos.org/data/hfrnet/). Funding for this work was provided by National Science Foundation, grants OCE-0961725 and OCE-1155855, to D.L.V. S.D.M. was funded by a Ford Foundation Predoctoral Fellowship.

References

Adams, M. M., A. L. Hoarfrost, A. Bose, S. B. Joye, and P. R. Girguis (2013), Anaerobic oxidation of short-chain alkanes in hydrothermal sediments: Potential influences on sulfur cycling and microbial diversity, *Frontiers Microbiol.*, *4*, doi:10.3389/fmicb.2013.00110.

Arp, D. J. (1999), Butane metabolism by butane-grown 'Pseudomonas butanovora', *Microbiology*, *145*(5), 1173–1180.

Ashraf, W., A. Mihdhir, and C. J. Murrell (1994), Bacterial oxidation of propane, *FEMS Microbiol. Lett.*, *122*(1), 1–6.

Beckenbach, E. (2004), Surface circulation in the Santa Barbara Channel: An application of high frequency radar for descriptive physical oceanography in the coastal zone, PhD thesis, Univ. of Calif., Santa Barbara.

Bottinga, Y. (1969), Calculated fractionation factors for carbon and hydrogen isotope exchange in the system calcite-carbon dioxide-graphite-methane-hydrogen-water vapor, *Geochim. Cosmochim. Acta*, *33*(1), 49–64.

Cicerone, R. J., and R. S. Oremland (1988), Biogeochemical aspects of atmospheric methane, *Global Biogeochem. Cycles*, *2*(4), 299–327.

Clark, J., L. Washburn, J. S. Hornafius, and B. P. Luyendyk (2000), Dissolved hydrocarbon flux from natural marine seeps to the southern California Bight, *J. Geophys. Res.*, *105*(C5), 11,509–11,522.

Coast Guard, United States (2013), Oil pollution act liability limits in 2013, pp. 1–28, Washington, D. C. [Available at: http://www.uscg.mil/npfc/docs/PDFs/Reports/Liability_Limits_Report_2013.pdf.]

Collins, W., R. Derwent, C. Johnson, and D. Stevenson (2002), The oxidation of organic compounds in the troposphere and their global warming potentials, *Clim. Change*, *52*, 453–479.

Du, M., and J. D. Kessler (2012), Assessment of the spatial and temporal variability of bulk hydrocarbon respiration following the Deepwater Horizon oil spill, *Environ. Sci. Technol.*, *46*(19), 10,499–10,507.

Etiope, G., K. R. Lassey, R. W. Klusman, and E. Boschi (2008), Reappraisal of the fossil methane budget and related emission from geologic sources, *J. Geophys. Res.*, *35*, L09307, doi:10.1029/2008GL033623.

Fung, I., J. John, J. Lerner, E. Matthews, M. Prather, L. P. Steele, and P. J. Fraser (1991), Three-dimensional model synthesis of the global methane cycle, *J. Geophys. Res.*, *96*(D7), 13,033–13,065.

Griffiths, R. D., B. A. Caldwell, J. D. Cline, W. A. Broich, and R. Y. Morita (1982), Field observations of methane concentrations and oxidation rates in the southeastern Bering Sea, *Appl. Environ. Microbiol.*, *44*, 436–446.

Halewood, E. R., C. A. Carlson, M. A. Brzezinski, D. C. Reed, and J. Goodman (2012), Annual cycle of organic matter partitioning and its availability to bacteria across the Santa Barbara Channel continental shelf, *Aquat. Microb. Ecol.*, *67*, 189–209.

Hanson, R. S., and T. E. Hanson (1996), Methanotrophic bacteria, *Microbiol. Rev.*, *60*(2), 439–471.

Harayama, S., H. Kishira, Y. Kasai, and K. Shutsubo (1999), Petroleum biodegradation in marine environments, *J. Mol. Microbiol. Biotechnol.*, *1*(1), 63–70.

Harms, S., and C. D. Winant (1998), Characteristic patterns of the circulation in the Santa Barbara Channel, *J. Geophys. Res.*, *103*(C2), 3041–3065.

Heintz, M. B., S. Mau, and D. L. Valentine (2012), Physical control on methanotrophic potential in waters of the Santa Monica Basin, Southern California, *Limnol. Oceanogr.*, *57*(2), 420–432, doi:10.4319/lo.2012.57.2.0420.

Horibe, Y., and H. Craig (1995), DH fractionation in the system methane-hydrogen-water, *Geochim. Cosmochim. Acta*, *59*(24), 5209–5217.

Hornafius, J. S., D. C. Quigley, and B. P. Luyendyk (1999), The world's most spectacular marine hydrocarbon seeps (Coal Oil Point, Santa Barbara Channel, California): Quantification of emission, *J. Geophys. Res.*, *104*(C9), 20,703–20,711.

Jacob, D. J., B. D. Field, E. M. Jin, I. Bey, Q. Li, J. A. Logan, R. M. Yantosca, and H. B. Singh (2002), Atmospheric budget of acetone, *J. Geophys. Res.*, *107*(D10), doi:10.1029/2001JD000694.

Katzenstein, A. S., L. A. Doezema, I. J. Simpson, D. R. Blake, and F. S. Rowland (2003), Extensive regional atmospheric hydrocarbon pollution in the southwestern United States, *Proc. Natl. Acad. Sci. U. S. A.*, *100*(21), 11,975–11,979.

Kessler, et al. (2011), A persistent oxygen anomaly reveals the fate of spilled methane in the deep Gulf of Mexico, *Science*, *331*(6015), 312–315.

Kinnaman, F. S., D. L. Valentine and S. C. Tyler (2007), Carbon and hydrogen isotope fractionation associated with the aerobic microbial oxidation of methane, ethane, propane and butane, *Geochim. Cosmochim. Acta*, *71*, 271–283.

Kniemeyer, O., F. Musat, S.M. Sievert, K. Knittel, H. Wilkes, M. Blumenberg, W. Michaelis, A. Classen, C. Bolm, S.B. Joye, and F. Widdel (2007), Anaerobic oxidation of short-chain hydrocarbons by marine sulphate-reducing bacteria, *Nature*. *449*(7164), 898–901.

Margesin, R., and F. Schinner (1999), Biological decontamination of oil spills in cold environments, *J. Chem. Technol. Biotechnol.*, *74*(5), 381–389.

Mastalerz, V., G. J. De Lange, and A. Dählmann (2009), Differential aerobic and anaerobic oxidation of hydrocarbon gases discharged at mud volcanoes in the Nile deep-sea fan, *Geochim. Cosmochim. Acta*, *73*(13), 3849–3863.

Mau, S., D. L. Valentine, J. F. Clark, J. Reed, R. Camilli and L. Washburn (2007), Dissolved methane distributions and air-sea flux in the plume of a massive seep field, Coal Oil Point, California, *Geophys. Res. Lett.*, *34*, L22603, doi:10.1029/2007GL031344.

Mau, S., M. B. Heintz, F. S. Kinnaman, and D. L. Valentine (2010), Compositional variability and air-sea flux of ethane and propane in the plume of a large, marine seep field near Coal Oil Point, CA, *Geo Mar. Lett.*, *30*(3–4), 367–378.

Mau, S., J. Blees, E. Helmke, H. Niemann, and E. Damm (2013), Vertical distribution of methane oxidation and methanotrophic response to elevated methane concentrations in stratified waters of the Arctic fjord Storfjorden (Svalbard, Norway), *Biogeosciences*, *10*, 6267–6278.

Olszowy, H., and W. Kitching (1984), Stereochemistry of trifluoroacetolysis and brominolysis of the cyclohexyl-tin bond, *Organometallics*, *3*(11), 1676–1683.

Pack, M. A., M. B. Heintz, W. S. Reeburgh, S. E. Trumbore, D. L. Valentine, X. Xu and E. R. Druffel (2011), A method for measuring methane oxidation rates using low-levels of 14C-labeled methane and accelerator mass spectrometry, *Limnol. Oceanogr. Methods*, *9*, 245–260.

Perry, J. (1980), Propane utilization by microorganisms, *Adv. Appl. Microbiol.*, *26*, 89–115.

Plass-Dulmer, C., R. Koppmann, M. Ratte, and J. Rudolph (1995), Light nonmethane hydrocarbons in seawater, *Global Biogeochem. Cycles*, *9*(1), 79–100.

Quistad, S. D., and D. L. Valentine (2011), Anaerobic propane oxidation in marine hydrocarbon seep sediments, *Geochim. Cosmochim. Acta*, *75*(8), 2159–2169.

Reddy, C. M., et al. (2012), Composition and fate of gas and oil released to the water column during the Deepwater Horizon oil spill, *Proc. Natl. Acad. Sci. U. S. A.*, *109*(50), 20,229–20,234.

Redmond, M. C., and D. L. Valentine (2012), Natural gas and temperature structured a microbial community response to the Deepwater Horizon oil spill, *Proc. Natl. Acad. Sci. U. S. A.*, *109*(50), 20,292–20,297, doi:10.1073/pnas.1108756108.

Redmond, M. C., D. L. Valentine, and A. L. Sessions (2010), Identification of novel methane-, ethane-, and propane-oxidizing bacteria at marine hydrocarbon seeps by stable isotope probing, *Appl. Environ. Microbiol.*, *76*(19), 6412–6422.

Reeburgh, W. S. (1969), Observations of gases in Chesapeake Bay sediments, *Limnol. Oceanogr.*, *14*(3), 368–375.
Reeburgh, W. S. (1983), Rates of biogeochemical processes in anoxic sediments, *Annu. Rev. Earth Planet. Sci.*, *11*(1), 269–298.
Reeburgh, W. S. (2007), Oceanic methane biogeochemistry, *Chem. Rev.*, *107*, 486–513.
Reeburgh, W. S., B. B. Ward, S. C. Whalen, K. A. Sandbeck, K. A. Kilpatrickt and L. J. Kerkhof (1991), Black Sea methane geochemistry, *Deep Sea Res., Part A*, *38*, S1189–S1210.
Singh, H. B., D. O'hara, D. Herlth, W. Sachse, D. R. Blake, J. D. Bradshaw, M. Kanakidou, and P. J. Crutzen (1994), Acetone in the atmosphere: Distribution, sources, and sinks, *J. Geophys. Res.*, *99*(D1), 1805–1819.
Valentine, D. L. (2011), Emerging topics in marine methane biogeochemistry, *Annu. Rev. Mar. Sci.*, *3*(1), 147–171, doi:10.1146/annurev-marine-120709-142734.
Valentine, D. L., D. Blanton, W. S. Reeburgh and M. Kastner (2001), Water column methane oxidation adjacent to an area of active hydrate dissociation, Eel River Basin, *Geochim. Cosmochim. Acta*, *65*(16), 2633–2640.
Valentine, D. L., et al. (2010), Propane respiration jump-starts microbial response to a deep oil spill, *Science*, *330*(6001), 208–211, doi: 10.1126/science.1196830.
Ward, B. B., K. A. Kilpatrick, P. C. Novelli, and M. I. Scranton (1987), Methane oxidation and methane fluxes in the ocean surface layer and deep anoxic waters, *Nature*, *327*(6119), 226–229.